

A Study of the Dynamic Properties of the Human Red Blood Cell Membrane Using Quasi-Elastic Light-Scattering Spectroscopy

Roy B. Tishler and Francis D. Carlson

The Thomas C. Jenkins Department of Biophysics, Johns Hopkins University, Baltimore, Maryland 21218 USA

ABSTRACT A quasi-elastic light-scattering (QELS) microscope spectrometer was used to study the dynamic properties of the membrane/cytoskeleton of individual human red blood cells (RBCs). QELS is a spectroscopic technique that measures intensity fluctuations of laser light scattered from a sample. The intensity fluctuations were analyzed using power spectra and the intensity autocorrelation function, $g^{(2)}(\tau)$, which was approximated with a single exponential. The value of the correlation time, T_{corr} , was used for comparing results. Motion of the RBC membrane/cytoskeleton was previously identified as the source of the QELS signal from the RBC (R. B. Tishler and F. D. Carlson. 1987. *Biophys. J.* 51:993–997), and additional data supporting that conclusion are presented. Similar results were obtained from anucleate mammalian RBCs that have structures similar to that of the human RBC, but not for morphologically distinct, nucleated RBCs. The effect of altering the physical properties of the cytoplasm and the membrane/cytoskeleton was also studied. Osmotically increasing the cytoplasmic viscosity led to significant increases in T_{corr} . Increasing the membrane cholesterol content and increasing the intracellular calcium content both led to decreased deformability of the human RBC. In both cases, the modified cells with decreased deformability showed an increase in T_{corr} , demonstrating that QELS could measure biochemically induced changes of the membrane/cytoskeleton. Physiological changes were measured in studies of age-separated RBC populations which showed that T_{corr} was increased in the older, less deformable cells.

INTRODUCTION

Measurement of the dynamic properties of a cell can provide important information on its physical state. The dynamics of certain types of motion of a cell and/or its structural components can be inferred from the measurement of the intensity fluctuations in light scattered by the cell. Changes in cellular dynamics, which reflect alterations in the physical properties of the cell arising from biochemical modifications or physiological changes, lead to changes in the temporal properties of the intensity fluctuations.

Quasi-elastic light scattering (QELS) is a spectroscopic technique that measures fluctuations in scattered light intensity arising from the motion of a sample. Motion of the membrane/cytoskeleton has been previously shown (Tishler and Carlson, 1987) to be the primary source of the QELS signal from human red blood cells (RBC). QELS was used to measure the dynamic properties of the membrane/cytoskeleton of human RBCs under a variety of experimental conditions. This technique offers a rapid, noninvasive way to monitor membrane motion of an individual cell and, as we will show, to study the effects of biochemical manipulations and physiological changes. A QELS microscope spectrometer (Blank et al., 1987), which allows measurements to be made on single cells, was used in all experiments. Intensity fluctuations of the scattered light were characterized using both autocorrelation function and spectral analysis. The autocorrelation data were analyzed as described previously (Tishler and Carlson, 1987) using the intensity autocorrela-

tion function, $g^{(2)}(\tau)$, defined as

$$g^{(2)}(\tau) = \langle I(t)I(t + \tau) \rangle / \langle I(t) \rangle^2,$$

where τ is the delay time, $I(t)$ is the instantaneous intensity, and $\langle \dots \rangle$ represents the time average. In the case where $g^{(2)}(\tau)$ decays exponentially (e.g., freely diffusing particles small compared with the wavelength of light), it has the following form:

$$g^{(2)}(\tau) = 1 + Ae^{-\tau/T_{\text{corr}}}.$$

T_{corr} is the correlation time of the signal, and A is the amplitude of the autocorrelation function and is an instrumental constant that is also influenced by details of the sample scattering. The autocorrelation function measured from an RBC is a more complex process than this but was analyzed using this functional form in order to facilitate comparison of the data.

The human red blood cell is a relatively simple cellular system. Its two major components are cytoplasm, which is essentially a concentrated hemoglobin (Hb) solution, and a thin membrane/cytoskeleton that surrounds the cytoplasm. The dynamic state of both components can contribute to light scattering fluctuations: (a) Hb diffuses and (b) spontaneous fluctuations of the membrane/cytoskeleton lead to changes in cell shape. The optical manifestations of the cell shape changes are referred to as the "flicker phenomenon" (Blowers et al., 1950).

Previous QELS studies of individual RBCs have been interpreted in terms of a pure Hb source (Nishio et al., 1983), in terms of a combined Hb/membrane signal that emphasizes the Hb contribution (Nishio et al., 1985; Peetermans et al., 1986), and in terms of a primarily membrane/cytoskeleton contribution (Tishler and Carlson, 1987). This paper will

Received for publication 5 May 1992 and in final form 22 September 1993.

Address reprint requests to Dr. Roy B. Tishler, Joint Center for Radiation Therapy, 50 Binney Street, Boston, MA 02115.

© 1993 by the Biophysical Society

0006-3495/93/12/2586/15 \$2.00

expand on the data showing the membrane/cytoskeleton to be the origin of the QELS signal and will present power spectra of the scattered light.

The QELS signal will be shown to be sensitive to alterations in the physical properties of the cell. Two biochemical modifications, increasing the membrane cholesterol level and increasing the intracellular calcium concentration, have been shown to decrease the deformability of the RBC, primarily through an effect on the membrane. Both lead to measurable changes in $g^{(2)}(\tau)$ with the mean correlation time, T_{corr} , increasing in the less deformable cells. Increasing the buffer osmotic strength leads to an increase in cytoplasmic viscosity and a decrease in cell deformability. T_{corr} also increases under these conditions. The relationship between alterations in the physical properties of the cell and changes in $g^{(2)}(\tau)$ allowed QELS to be used to detect physiological membrane changes associated with aging of the RBC.

MATERIALS AND METHODS

Human sample preparation

Human blood samples were obtained by venipuncture from a 25–27-year-old male using acid-citrate-dextrose as the anticoagulant. After removal of the plasma and “buffy coat,” cells were washed three times in an iso-osmotic HEPES-Ringers buffer (Schindler et al., 1980). Following the final wash the RBCs were resuspended in HEPES-Ringers with 1 mg/ml of bovine serum albumin (BSA). The final dilution of the RBC pellet ranged from 1:5,000 to 1:50,000, which was sufficient to separate individual RBCs by several cell diameters on the microscope slide. Red blood cell ghosts were prepared from these samples by hemolysis, using a standard procedure (Lin and Snyder, 1977).

Hypertonic buffers were prepared by adding various salts, at a concentration of 225 mM (1.5× isotonic), to an isotonic HEPES-Ringers solution with BSA, and the pH was readjusted to 7.4. These solutions therefore had a total osmotic strength of 2.5× isotonic. The concentrated RBCs were diluted 1:100,000 with the buffer prior to light scattering studies.

Alteration of membrane cholesterol level

The cholesterol level of the RBC membrane was altered following the standard methods of Cooper et al. (1975) and Hui et al. (1980). Lipid/cholesterol dispersions were made from solutions containing 40 mg D,L- α -phosphatidyl choline dipalmitoyl and either 23 or 80 mg of cholesterol in 10 ml of 155 mM NaCl, giving cholesterol/phospholipid values of 1.1 or 3.8, respectively. Following sonication, the dispersions were centrifuged at 30,000 × g for 30 min. A 10% RBC suspension was prepared in HEPES-Ringers containing 1 mg/ml glucose and 1000 units/ml penicillin (Pen-G). Four ml of the RBC suspension and 4 ml of a lipid/serum solution (1.3 ml heat-treated serum and 2.7 ml phospholipid/cholesterol dispersion) were incubated for 24–48 h at 37°C and frequently resuspended. After incubation, the cells were separated from the lipid/cholesterol dispersion and washed three times in HEPES-Ringers with glucose and Pen-G. Each RBC pellet was resuspended in 1 ml of HEPES-Ringers with BSA and Pen-G and then diluted 1:100 in the same buffer.

Alteration of intracellular calcium levels

The intracellular calcium concentration of the RBC was altered by using the ionophore A23187 based on the methods of Lorand et al. (1978). RBCs were washed three times in phosphate-buffered saline (pH 7.4) and then suspended at 10% concentration in a buffer containing 100 mM KCl, 60 mM NaCl, 10 mM glucose, 5 mM Tris-HCl, 100 units/ml Pen-G, 20 μ M calcium-

A23187 (Sigma C9275), and 1 mM CaCl₂. In one of the controls the buffer contained 20 μ M magnesium-A23187 and 1 mM MgCl₂ in place of the calcium compounds. In another control the same concentrations of magnesium-A23187 and MgCl₂ were used, but 1 mM EGTA was added. A third control used a buffer without a divalent cation or ionophore. The cell suspensions were incubated in a 37°C water bath for 20 h and were resuspended every few hours. Following incubation the cells were resuspended and diluted 1:1000 into buffer with 1 mg/ml BSA added.

Preparation of age-separated cells

The increase in density that occurs as the RBCs become older allows age-separated populations to be prepared. If only extremes of densities are examined, a reasonable separation in terms of age can be expected (Sutera et al., 1985). Cell populations of different ages were obtained using the density gradient centrifugation technique of Vettore et al. (1980) with minor modifications. A density-gradient mixture was prepared that consisted of 35% colloidal silica particles coated with polyvinylpyrrolidone (Percoll; Pharmacia Fine Chemicals AB, Uppsala, Sweden), 20% meglamine diatrizoate (Renografin 60; E. R. Squibb and Sons, New York), and 45% distilled water. Nine ml of the density gradient mixture and 0.5 ml of blood filtered through nylon were placed in 10-ml ultracentrifuge tubes. This mixture was centrifuged at 27,000 × g for 20 min. Following centrifugation, the top and bottom cell layers were removed and washed four times in iso-osmotic saline at pH 7.4. The cells were then diluted with iso-osmotic saline and BSA for QELS studies.

Red blood cells from different species

Samples of rat and dog blood were obtained from animals being used for respiratory studies at the Johns Hopkins School of Public Health. Chicken blood was collected at the Dover Poultry Company (Baltimore, MD). Acid-citrate-dextrose was used as the anticoagulant for these samples. The National Aquarium in Baltimore supplied samples from Beluga whales and harbor seals. The Baltimore Zoo provided blood samples from a jungle cat and an antelope. These samples were drawn into “purple top” vacuum tubes, which contained citrate as the anticoagulant.

The above samples were prepared using the HEPES-Ringer buffer and the standard human sample preparation technique. For the jungle cat, whale, and seal samples, the procedure was modified slightly due to the small volumes of the samples.

Blood from a toad (*Bufo marinus*) was prepared with an anticoagulant (Sheif and Wensink, 1981) and diluted in a frog HEPES-Ringer buffer (100 mM NaCl, 10 mM NaHEPES, 4 mM KCl, 1 mM CaCl₂, 0.7 mM NaH₂PO₄, 0.6 mM MgSO₄, and 5 mM glucose). The preparation procedure used was the same as for the human samples, but smaller volumes were employed.

Experimental apparatus

Quasi-elastic light-scattering microscope

All measurements were made using a QELS microscope spectrometer based on a Nikon Diaphot inverted microscope with a HeNe laser (Blank et al., 1987). For the experiments described here, a 330- μ m front aperture and a 250- μ m back aperture were used with a 40× long working distance phase objective (Nikon 40 DL, NA 0.55). Under these conditions, the scattering volume has an 8- μ m-diameter cross section, and the spread in scattering angles is $\pm 5.5^\circ$. Details of the photon detection technique have been presented previously (Blank et al., 1987).

Sample holders

For experiments with scattering angles below 42°, a microscope slide and coverslip sealed with petroleum jelly were used as the scattering chamber. For scattering angles above 42°, a standard (1 × 1 × 3 cm) optical cuvette

lying on its side was used as a scattering chamber. In both cases cell suspensions were allowed to settle so that measurements were made on RBCs lying flat on the horizontal surface of the sample holder. For the microscope slide holder, the light was incident on the top surface of the coverslip, whereas for the cuvette it was incident on the side of the cuvette. Thus for both sample holders, the incident beam crossed an air/glass interface at a non-normal angle, and corrections for refractive effects were made. Scattered light was collected from light leaving the bottom of both sample holders normal to the surface, so no angular correction was required. For all experiments, cells were allowed to settle on the bottom of the cuvette/coverslip prior to measurements. RBCs that were biconcave disks were chosen at random for measurements.

Data collection and analysis

Pulses from the amplifier-discriminator were processed with an autocorrelator-multiscaler (Haskell and Carlson, 1980) interfaced to a Plessey 11/23 digital computer containing an 11/73 processor running under the UNIX operating system.

Autocorrelator

The autocorrelator calculated the one-bit-scaled autocorrelation function (acf) in real time (Haskell and Carlson, 1980). With the appropriate choice of scaling levels, this gives an excellent estimate of the true intensity acf (Jakeman et al., 1972). For all experiments described these conditions were maintained. The quantity calculated by the autocorrelator was the intensity acf, $G^{(2)}(\tau)$, defined as

$$G^{(2)}(\tau) = \langle n(t)n(t + \tau) \rangle$$

where $n(t)$ represents the number of counts in a sample time.

The normalized intensity autocorrelation function, $g^{(2)}(\tau)$, was derived from $G^{(2)}(\tau)$:

$$g^{(2)}(\tau) = G^{(2)}(\tau) / \langle n(t) \rangle^2$$

where $\langle n(t) \rangle$ is the number of photon counts per experiment. Each measurement of $G^{(2)}(\tau)$ was normalized by the mean number of counts for that particular measurement in order to minimize the effects of variations in the laser power or the sample from one determination to the next (Oliver, 1974). In a typical experiment, five sets of data were collected consecutively for each RBC. Each data set represented a measurement of $G^{(2)}(\tau)$, which was accumulated in real time and then transferred to the computer. The subsequent data analysis was performed off-line. The normalized intensity acf, $g^{(2)}(\tau)$, is the quantity used for data analysis.

The sampling of $G^{(2)}(\tau)$, and thus the range of correlation times probed, was varied in two ways. The correlator sample times were changed over a

range of 6 μ s to 4 ms. In addition, there were two sampling modes of the correlator. In the linear mode the 40 data channels collected photon counts in 40 consecutive sample times of equal duration. The parabolic mode gave a 40-channel acf in five groups of 8 channels. The first 8 channels were each 1 sample time apart, the next 8 were 2 apart, the next 8 were 4 apart, the next 8 were 8 apart, and the last 8 were 16 apart. This sampling allowed a range of 248 sample times to be studied while maintaining high resolution at shorter delay times.

A single exponential fit gave a quantitative description of $g^{(2)}(\tau)$ in terms of two parameters: the amplitude of the autocorrelation function and the correlation time. An important aspect of the fitting procedure was that the background (i.e., the level to which $G^{(2)}(\tau)$ decayed for long delay times) was a calculated parameter. The single exponential fit was used to describe $g^{(2)}(\tau)$, although the autocorrelation function was a mixture of multiple components. The amplitude of the single exponential fit is its value for $\tau = 0$ and will be referred to as $g^{(2)}(0)-1$. The correlation time, T_{corr} , of the exponential fit is an average of the correlation times present in $g^{(2)}(\tau)$.

Comparisons of autocorrelation function

Data from groups of cells were compared in order to determine if different preparation procedures altered the QELS signal, as measured by T_{corr} . The parameters used for these comparisons were the mean of the values of T_{corr} calculated from the individual cells in a group and the SD of this mean. T_{corr} for a particular cell was typically the average of five consecutive measurements of $g^{(2)}(\tau)$. If the mean value of T_{corr} from a particular cell differed from the mean value for the group of cells from which it was taken by more than 3 SDs, data from that cell were excluded from computation of the mean value for the group. The data from two groups of cells were compared using a modified Student's t distribution, which allowed for a different number of cells and different SDs of the mean for each group (Cochran, 1964; Snedecor and Cochran, 1967, section 4.14). Two samples were said to differ if $p < 0.05$.

Data from the RBC ghosts were approached differently than data from other modified RBC samples. The reasons for this are twofold: (i) as a result of the decreased scattering intensity from the ghosts, these data can be markedly altered if there is interference from dust, and (ii) the process of forming ghosts may damage some cells. The mean value of T_{corr} for a group of ghosts was calculated, excluding extreme values as follows: data from a particular ghost were excluded if (a) for that cell the mean value of the five determinations of T_{corr} was less than the SD of those five measurements or (b) if the value of T_{corr} for a particular cell was greater than 3 SDs above the mean for the group of cells from which it was taken.

Measurements from RBCs showed there was no angular dependence of T_{corr} at a given sample time (Tishler and Carlson, 1987; this paper, Table 1). Data from a single angle were used for comparison studies, and no further investigation of angular dependence was performed for modified cells. Most

TABLE 1 Correlation times and amplitudes of autocorrelation functions from red blood cells using different scattering angles and sample times

Sample time	$\theta = 31^\circ$ ($n = 3$)		$\theta = 40^\circ$ ($n = 5$)		$\theta = 63^\circ$ ($n = 4$)		$\theta = 83^\circ$ ($n = 4$)	
	T_{corr}	$g^{(2)}(0)-1$	T_{corr}	$g^{(2)}(0)-1$	T_{corr}	$g^{(2)}(0)-1$	T_{corr}	$g^{(2)}(0)-1$
6 μ s, P	4.7 \pm 1.9	3.1 \pm 0.4	6.0 \pm 1.6	5.9 \pm 0.9	6.9 \pm 2.3	10.6 \pm 2.0	5.2 \pm 1.7	10.6 \pm 0.6
40 μ s, P	16.9 \pm 4.4	2.5 \pm 0.7	18.7 \pm 4.1	4.9 \pm 0.9	23.2 \pm 4.2	10.4 \pm 1.7	21.8 \pm 5.6	10.2 \pm 1.8
150 μ s, P	37.2 \pm 7.3	2.4 \pm 0.8	40.6 \pm 10.6	4.7 \pm 1.8	53.5 \pm 10.5	9.2 \pm 1.7	44.5 \pm 6.1	8.8 \pm 1.9
1 ms, L	53 \pm 11	2.0 \pm 0.8	67 \pm 15	3.9 \pm 1.5	67 \pm 10	7.8 \pm 1.4	66 \pm 10	7.7 \pm 4.3
4 ms, L	175 \pm 48	1.4 \pm 0.7	208 \pm 37	3.4 \pm 2.0	180 \pm 17	6.1 \pm 1.4	169 \pm 18	6.6 \pm 1.4
4 ms, P	504 \pm 82	1.3 \pm 0.6	642 \pm 184	3.5 \pm 1.4	556 \pm 109	5.8 \pm 1.2	413 \pm 72	5.6 \pm 0.8

Results of single exponential fit of autocorrelation function measured from single RBCs acquired at a range of angles and sample times, using either the linear (L) or parabolic (P) mode (see text). The autocorrelation functions analyzed for each cell represent the average of 5 measurements of 100-s duration. The number of cells analyzed at each angle and sample time is noted. The errors represent the SD of the mean value, which was obtained by averaging the results from individual cells. Values for T_{corr} are expressed in milliseconds, and the values of $g^{(2)}(0)-1$ are shown $\times 100$. There were no significant differences between the values for T_{corr} measured at different scattering angles using a particular sample time.

data were collected using a 1-ms sample time, and manipulations of the RBC that primarily affected the membrane/cytoskeleton were studied. Although other interpretations regarding the source of the QELS signal at short delay times (sample time of $\sim 40 \mu\text{s}$) have been presented, as discussed below, the signal measured using a 1-ms sample time can be attributed only to membrane/cytoskeleton motion.

The method used to present the experimental data from individual cells was chosen to emphasize differences in the time dependence of $g^{(2)}(\tau)$. Data were presented in a "normalized" form (Fig. 3) with $g^{(2)}(\tau)-1$ being plotted with the highest channel set equal to 1 and other channels scaled appropriately. Data from Fig. 1 are presented in a non-normalized form, since the change in amplitude as a function of sample time is one of the factors being studied.

Calculation of power spectra

Multiscaler: time series data

The power spectrum of the scattered light was calculated from time series data collected with the same detection apparatus used for the autocorrelation functions, but with the autocorrelator used in the multiscaler mode. The time series obtained from the multiscaler contained gaps interspersed at regular intervals between the data. Artifacts created in the power spectrum due to these missed observations (Jones, 1962; Parzen, 1963) in the time series can be minimized by applying an appropriate correction to the data, which is most easily implemented using the autocorrelation function. The autocorrelation function was calculated by a two fold application of the fast Fourier transform (FFT) algorithm (Bloomfield, 1976; Cooley et al., 1977) to the time series data consisting of an array of 1024 points with zeros placed in the gaps of "missing observations." Each term of the autocorrelation function is multiplied by a correction factor (Jones, 1962; Parzen, 1963), which is determined by the length of the data gaps relative to the length of the data sets. A subsequent FT yields the power spectrum. For each spectrum shown here, data from 170 1024-point time series were combined.

RESULTS

I. Human red blood cell preparation: basic studies

The results of measurements of $g^{(2)}(\tau)$ from a single RBC, made using sample times from $6 \mu\text{s}$ to 4 ms, are shown in Fig. 1. Data from other cells were similar, although the precise value of $g^{(2)}(\tau)$ differed from cell to cell for a specific value of the delay time. The results of single exponential fits to data from this and other cells, collected using a range of scattering angles, are summarized in Table 1. These data yield estimates of the upper and lower limits of the correlation times present. The values of $g^{(2)}(\tau)$ obtained with a $6\text{-}\mu\text{s}$ sample time did not show a large increase as the delay time, τ , decreased to zero (Fig. 1 *a*), indicating that there was no major contribution from correlation times in the range of tens of microseconds. The mean correlation times from single exponential fits, measured using the $6\text{-}\mu\text{s}$ sample time, ranged from ~ 5 to 7 ms. The data obtained using the 4-ms sample time showed that the longest correlation times were in the range of hundreds of milliseconds. The average correlation time obtained from a single exponential fit was a strong function of the sample time used. However, for a given delay time, the values of $g^{(2)}(\tau)$ were independent of the sample time used. For example, data acquired using a $150\text{-}\mu\text{s}$ sample time in the parabolic mode (Fig. 1 *c*) and data collected with a 1-ms sample time in the linear mode (Fig. 1 *d*)

spanned the same range of delay times and were virtually superimposable.

The amplitude of the autocorrelation function, $g^{(2)}(0)-1$, decreased as the sample time was increased (Table 1). This result is expected for $g^{(2)}(\tau)$, which is made up of a broad distribution of correlation times. For longer sample times, contributions from the short correlation time components of $g^{(2)}(\tau)$ had decayed to a small fraction of their initial value within the first sample time. This feature of the data was present at all the scattering angles studied (Table 1). Another significant feature was the relatively low values of $g^{(2)}(0)-1$. The theoretical value of $g^{(2)}(0)-1$ for the aperture combination used was 0.77 (Saleh, 1978), and for a model system of polystyrene latex spheres, measured using the microscope apparatus, it was 0.72 ± 0.01 (Blank et al, 1987). Even for the shortest sample time examined, $g^{(2)}(0)-1$ measured for RBCs was in the range of 0.03 to 0.10. For a particular sample time, T_{corr} was essentially independent of the scattering angle, but there was a significant increase in $g^{(2)}(0)-1$ as the scattering angle was increased.

Power spectra computed using sample times ranging from 1 to 10 ms are shown in Fig. 2. All spectra contained a large low-frequency contribution that decayed monotonically. These low-frequency spectral components corresponded to the slowly decaying contributions seen in the autocorrelation functions. The half-width of the low frequency contribution decreased as the sample time was increased. This indicates that a different measurement of the power spectrum was obtained as the sample time was changed. This observation is similar to the changing values of the correlation time measured for autocorrelation functions using different sample times.

Table 2 summarizes results from ghost samples studied using sample times of $40 \mu\text{s}$ and 1 ms. Data from ghosts and intact cells were similar, but the ghost data showed slightly increased values of T_{corr} and exhibited a higher degree of variability. Data from ghosts were collected using longer experiment durations due to the decreased scattering intensity from the ghosts relative to intact RBCs.

II. Variations of ionic/osmotic conditions

The effect of increased NaCl concentration on $g^{(2)}(\tau)$ has been previously demonstrated (Tishler and Carlson, 1987). A number of additional salts were studied. These compounds were added to an isotonic buffer at a concentration of 225 mM ($1.5\times$ iso-osmotic), yielding a total osmotic strength of $2.5\times$ isosmotic. NaCl at this concentration had a large effect on $g^{(2)}(\tau)$ (Tishler and Carlson, 1987). The values of T_{corr} measured in the presence of ammonium chloride, where the cation and anion are permeant to the cell membrane (Hoerber, 1945; Jacobs and Stewart, 1947), did not differ from controls (Table 3). This result indicated that the changes seen with the NaCl were not due to an ionic strength effect. The absence of an effect on $g^{(2)}(\tau)$ by the ammonium chloride also indicated that this effect was not specific to the Cl^- ion. Choline chloride is similar to NaCl in that it has an impermeant cation

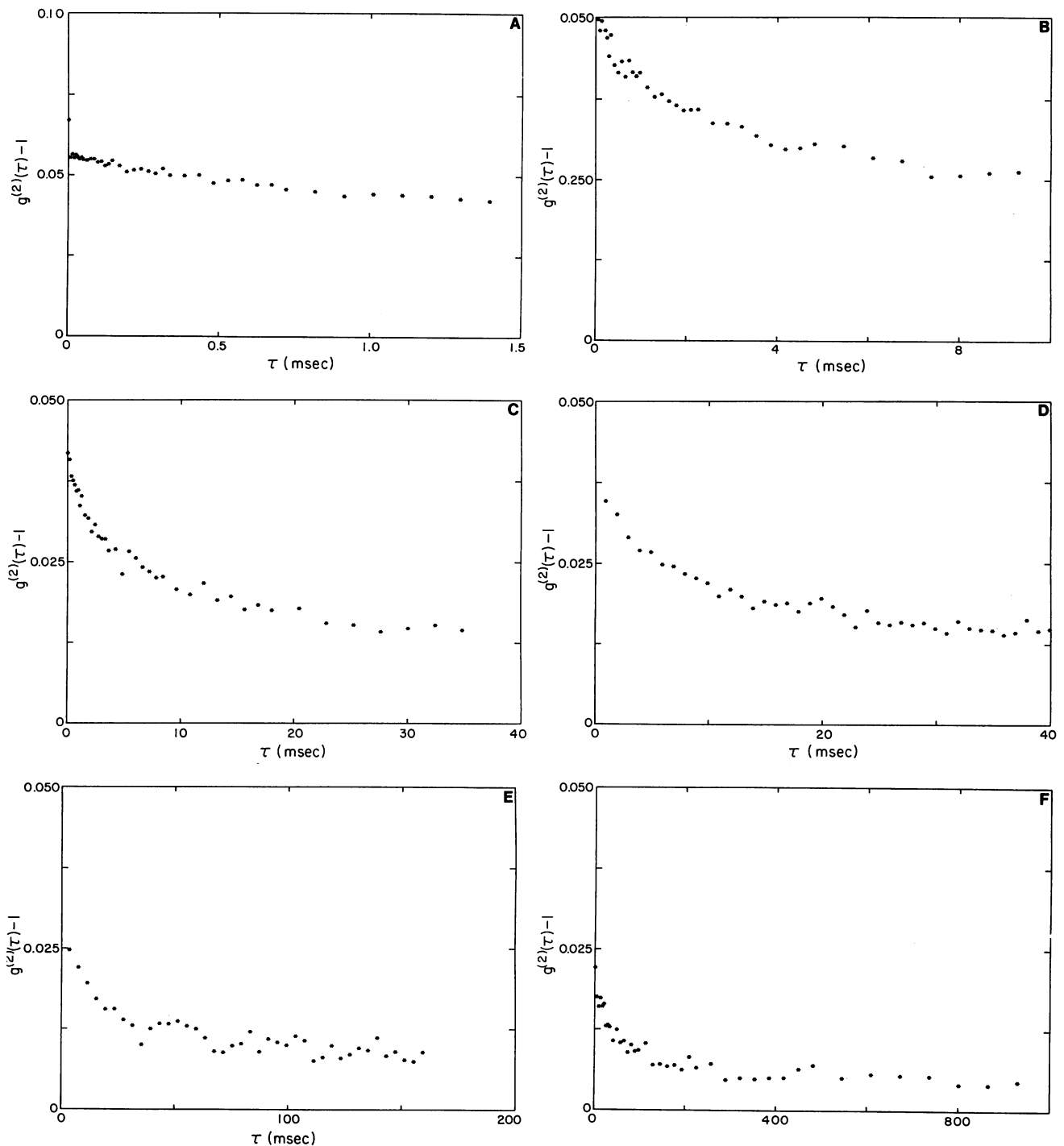


FIGURE 1 Autocorrelation functions for a range of sample times. Autocorrelation functions measured from a single cell using sample times from 6 μ s to 4 ms. Each graph represents the average of five 100-s determinations of $g^{(2)}(\tau)$. The results of single exponential fits to the average $g^{(2)}(\tau)$ (means plus or minus the SD values) are summarized below. $\theta = 42^\circ$. (a) Sample time = 6 μ s, parabolic mode. Increased counts in channel 1 are due to afterpulsing (Morton et al., 1967; Ford, 1985). $g^{(2)}(0)-1 = 0.056 \pm 0.002$. $T_{\text{corr}} = 4.1 \pm 0.2$ ms. (b) Sample time = 40 μ s, parabolic mode. $g^{(2)}(0)-1 = 0.046 \pm 0.002$. $T_{\text{corr}} = 12.7 \pm 0.4$ ms. (c) Sample time = 150 μ s, parabolic mode. $g^{(2)}(0)-1 = 0.035 \pm 0.001$. $T_{\text{corr}} = 27.4 \pm 0.7$ ms. (d) Sample time = 1 ms, linear mode. $g^{(2)}(0)-1 = 0.029 \pm 0.004$. $T_{\text{corr}} = 48 \pm 3$ ms. (e) Sample time = 4 ms, linear mode. $g^{(2)}(0)-1 = 0.019 \pm 0.003$. $T_{\text{corr}} = 164 \pm 7$ ms. (f) Sample time = 4 ms, parabolic mode. $g^{(2)}(0)-1 = 0.015 \pm 0.003$. $T_{\text{corr}} = 492 \pm 25$ ms.

and a permeable anion. Large increases in the correlation times were seen with choline chloride, demonstrating that the effect of NaCl was not specific to the Na^+ ion. Similar results were obtained when comparing the effect of sodium acetate and ammonium acetate on $g^{(2)}(\tau)$.

III. Red blood cells from different species

RBCs from a variety of species were examined to determine the extent to which measurements were characteristic of the RBCs themselves. These data showed that RBCs which are

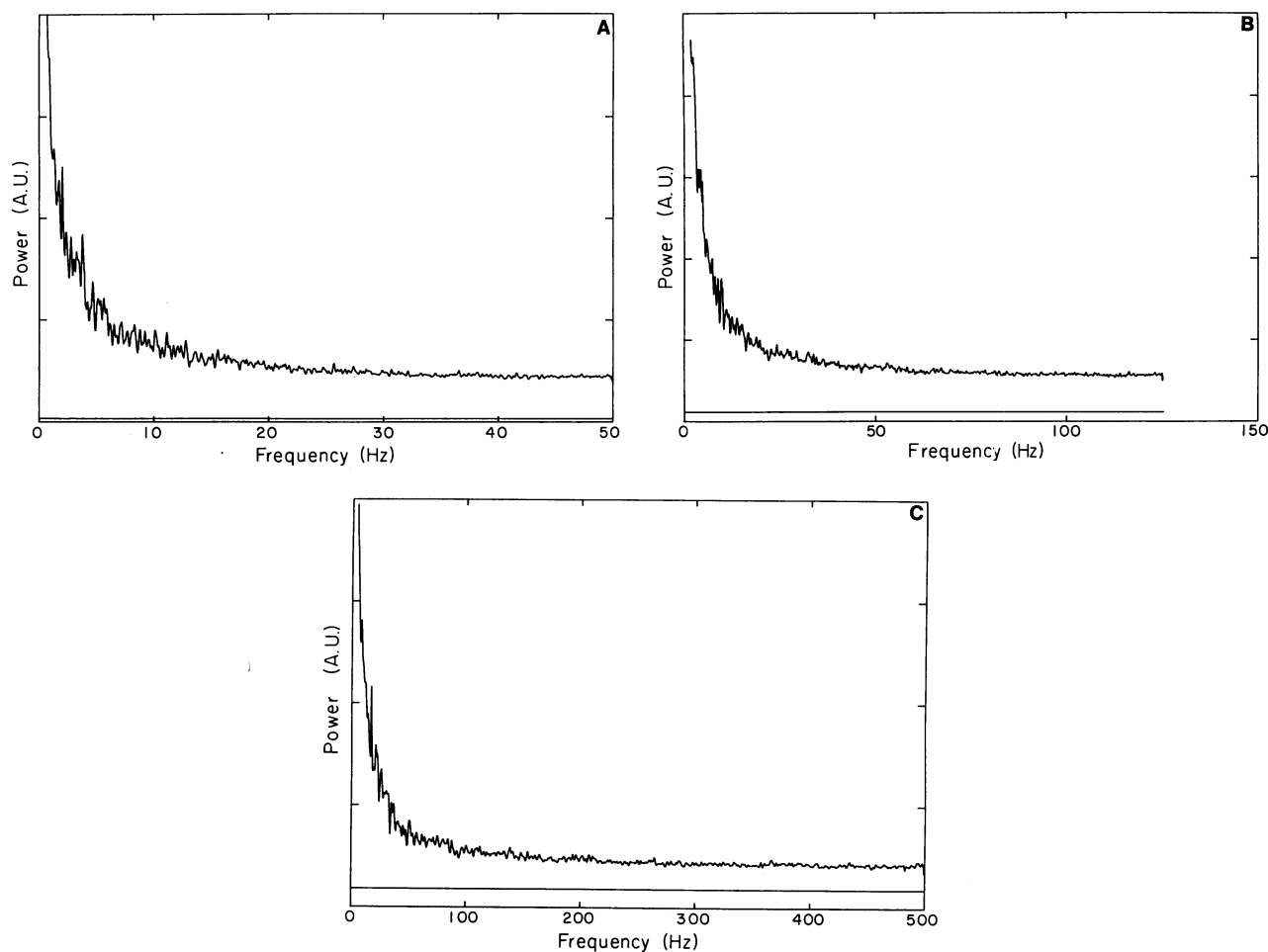


FIGURE 2 Power spectra for a range of sample times. Power spectra measured using a range of sample times. Each spectrum was calculated from 170 1024 point time series. The solid lines represent the power spectra calculated for a white noise source having the same count rate that was used in collecting the RBC spectrum. The spikes in a are artifacts arising from the missing observations in the time series. $\theta = 42^\circ$. (a) Sample time = 10 ms. (b) Sample time = 4 ms. (c) Sample time = 1 ms.

morphologically similar to human RBCs (anucleate, biconcave, mammalian RBCs) have very similar correlation times. The values for the nucleated RBCs, measured in the region of the nucleus, were two to three times higher than for the anucleate cells. The size and morphological features of RBCs from different species and the results from measurements made on them are summarized in Table 5. The values of T_{corr} were similar for the nucleated toad RBCs, measured in the region of the nucleus or the cell edge. However, the relative scattered intensity was decreased, and the values of $g^{(2)}(0)-1$ were increased in the region of the nucleus compared with the edge of the cell (data not shown).

IV. Membrane modifications

Representative data for experiments on cells with normal and increased levels of cholesterol are presented in Fig. 3. The cells with the higher cholesterol levels have a more slowly decaying $g^{(2)}(\tau)$ and thus larger values of T_{corr} . The values of T_{corr} are presented in histogram form along with data summaries (Fig. 4). The RBCs with increased membrane cholesterol levels showed 30–50% increases in T_{corr} relative to

cells with control levels of cholesterol. Although there is some overlap between the two groups of RBCs, they clearly represent different populations.

Changes in the intracellular calcium levels of the RBCs led to changes in T_{corr} . Cells treated with A23187 and 1 mM calcium showed increases in T_{corr} relative to controls (Table 4). Approximately 90% of the cells treated in this manner were crenated (echinocytes), but there was no difference in the values of T_{corr} between the echinocytes and biconcave disks. In both control experiments with magnesium compounds less than 20% of the cells were echinocytes. There were statistically insignificant increases in T_{corr} measured from the echinocytes relative to the biconcave disks. The calcium-treated cells had significant increases in T_{corr} relative to all three sets of controls (Table 4).

V. Age-separated red blood cells

The least and most dense fractions, which represent the youngest and oldest RBCs in a population, were used in the study of age-separated RBCs. The data from measurements on individual cells, along with a comparison of mean values

TABLE 2 Correlation times for red blood cell ghosts

Sample	T_{corr} (ms)	
	40 μs	1 ms
Ghosts	14.5 \pm 3.1 (3 of 4)	85 \pm 19 (4 of 4)
Ghosts	13.1 \pm 4.3 (5 of 6)	92 \pm 37 (6 of 8)
Ghosts	13.4 \pm 4.5 (3 of 3)	51 \pm 5 (4 of 4)
Ghosts	10.4 \pm 3.4 (7 of 8)	60 \pm 24 (8 of 8)
Ghosts	—	70 \pm 36 (6 of 7)
RBCs	9.8 \pm 1.0 (4)	46 \pm 6 (5)
RBCs	9.3 \pm 3.1 (8)	60 \pm 18 (8)
RBCs	9.8 \pm 4.5 (6)	—
RBCs	—	56 \pm 20 (15)

Summary of data collected from a number of ghost preparations for 40- μs and 1-ms sample times. Data presented are the mean and SDs as described in the text. The number of cells used for the calculations, as well as the total number originally in the group, are noted. For each individual ghost, five 300-s measurements of $g^{(2)}(\tau)$ were used. Results from separate experiments on intact RBCs, using five 60-s measurements, are included for purposes of comparison. All data collected with $\theta = 42^\circ$.

TABLE 3 Correlation times for red blood cells with different ionic compounds

Ionic compound	Permeable cation?	T_{corr} (ms)
N(CH ₃) ₄ Cl	No	710 \pm 440 (7)
Na(O ₂ CCH ₃)	No	440 \pm 160 (7)
NaCl	No	320 \pm 100 (6)
NH ₄ Cl	Yes	55 \pm 10 (13 of 15)
NH ₄ (O ₂ CHH ₃)	Yes	56 \pm 15 (6)
Control	—	66 \pm 16 (8)

Summary of data for cells with different ionic compounds added (at concentrations equivalent to 1.5 \times iso-osmotic) to iso-osmotic HEPES-Ringers. The data from all experiments using impermeable cations showed increased values of T_{corr} that were significantly different from the control group. Data from experiments with permeable cations were not significantly different from the controls. $\theta = 42^\circ$; sample time = 1 ms.

from the group, are presented as a histogram in Fig. 5. The older cells showed a significant ($p < 0.001$) increase in T_{corr} when compared with the younger cells.

DISCUSSION

Basic studies

Data supporting motion of the membrane/cytoskeleton as the primary source of the QELS signal from the human RBC have been presented previously (Tishler and Carlson, 1987). This paper expands on the previous work. The biochemical studies presented demonstrate the detection of membrane alterations by QELS.

Autocorrelation studies shown in Fig. 1 cover a larger range of sample times than previously presented. This shows the intensity fluctuations of the scattered light contain a broad range of decay times single exponential fits show values of T_{corr} from 4 to 600 ms. The autocorrelation function has decayed almost to baseline for the longest delay times shown. In contrast to this, QELS studies of white blood cells (Tishler

and Carlson, 1987 and unpublished data) show significant decays at delay times of up to 4 s with average values of T_{corr} as high as 3–5 s (using 100-ms sample times). Table 1 summarizes data from different RBCs and shows the lack of an angular dependence of T_{corr} for a particular sample time. However, as will be discussed below, there is a monotonic increase in $g^{(2)}(0)-1$ as the scattering angle increases.

The strongest evidence in support of the membrane/cytoskeleton as the primary source to the signal was the comparison of data from Hb and individual RBCs and ghosts (Tishler and Carlson, 1987). Data are presented from multiple cells in different groups of ghosts and RBCs (Table 2) which further demonstrates the similarity of the ghost and RBC data. A significant feature of the data was the increased variability, between groups of ghosts and between individual ghosts, indicating that these populations were more heterogeneous than the RBC populations. Since the formation of ghosts from RBCs by hypotonic hemolysis is a major perturbation that can lead to disruptions of the physical properties of the membrane/cytoskeleton (Kansu et al., 1980; Tanaka and Ohnishi, 1976), the increased heterogeneity of the ghost populations was not unexpected.

QELS studies of individual RBCs have been interpreted in terms of membrane motion (Tishler and Carlson, 1987) or a pure Hb contribution (Nishio et al., 1983). However, the actual data for $g^{(2)}(\tau)$ using a 40- μs sample time, which were used to support such disparate interpretations, were quite similar in terms of their time dependence. Nishio et al. (1985) and Peetermans et al. (1986) have subsequently interpreted data collected with a 40- μs sample time in terms of a combined Hb/membrane signal. An important consideration in the analysis is their difficulty in accurately representing the contribution due to the membrane/cytoskeleton. This problem is illustrated by the ghost data presented previously (Tishler and Carlson, 1987; Blank et al., 1986). Even for short sample times, some of the ghost and intact RBC data are almost indistinguishable. The mean values of T_{corr} for a

TABLE 4 Effects of altered intracellular calcium levels on correlation times

Divalent cation	Ionophore?	Cell morphology	T_{corr} (ms)
Ca ²⁺	Yes	Crenated	121 \pm 31 (11)
		Biconcave	115 \pm 25 (6)
Mg ²⁺	Yes	Crenated	83 \pm 17 (4)
		Biconcave	54 \pm 13 (5)
Mg ²⁺ (+EGTA)	Yes	Crenated	88 \pm 15 (3)
		Biconcave	52 \pm 2 (5)
—	No	Biconcave	66 \pm 15 (5)

Effect of changing intracellular calcium levels using the ionophore A23187. Calcium was present at a level of 1 mM in the incubating buffer. Control experiments included samples with magnesium at a concentration of 1 mM as the extracellular ion (with or without EGTA), and one sample was incubated without ionophore or divalent cation. Data from the calcium-treated cells were significantly different from the controls. There was no significant difference among the control groups. $\theta = 42^\circ$; sample time = 1 ms.

FIGURE 3. Representative data from cells with different cholesterol levels. Representative data from cells with normal and increased cholesterol levels. $g^{(2)}(\tau)$ from two cells in each group are plotted. Data are from five 60-s experiments on each cell. Data in upper group (X, O) are from cells with increased C/P ratios and data in lower group (*, +) are from cells with normal C/P ratios. $\theta = 42^\circ$, sample time 1 ms.

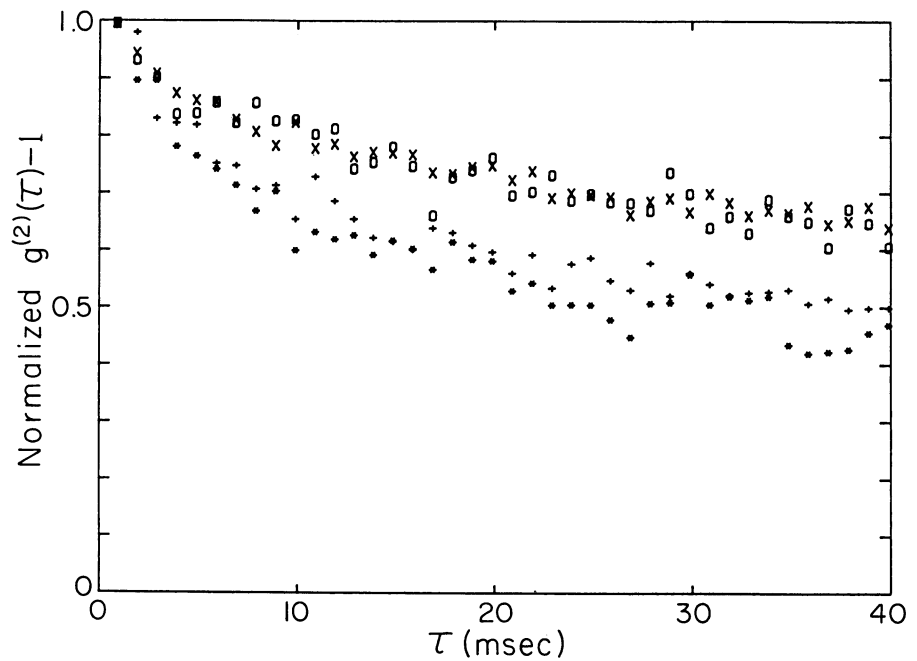
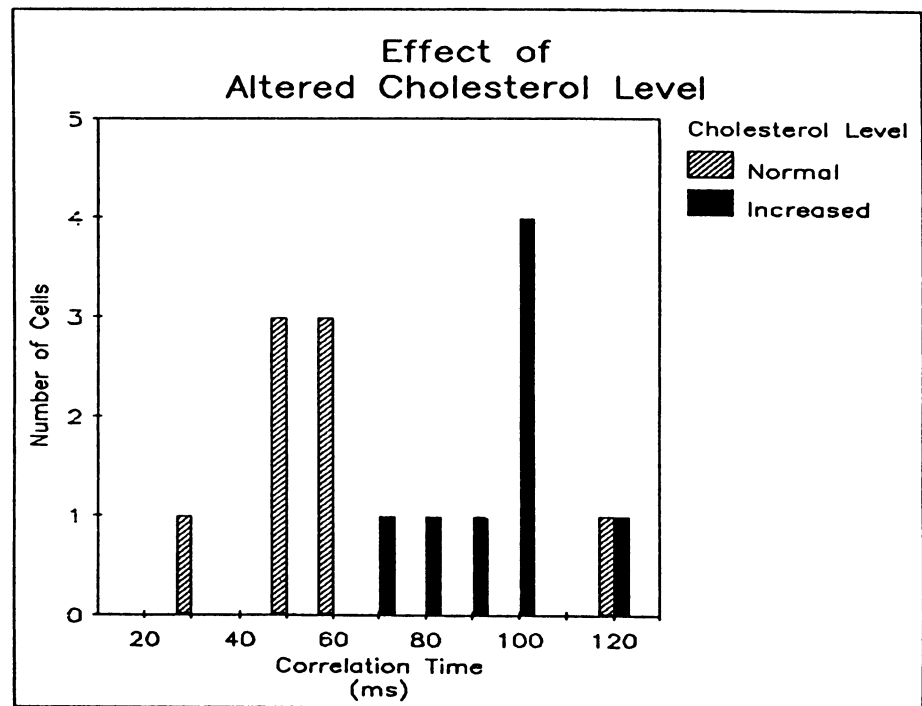


FIGURE 4. Distribution of correlation times for red blood cells with different cholesterol levels. Histograms of correlation times measured from RBCs incubated with cholesterol/phospholipid vesicles. The cells were incubated with vesicles which had a cholesterol to phospholipid ratio of 3.8 (increased cholesterol) or 1.1 (controls; this is approximately the value in a RBC membrane). Measurements were made on cells incubated with the vesicles for approximately 48 h. Data shown in histogram are values of T_{corr} obtained from $g^{(2)}(\tau)$ measured using a 1 ms sample time with $\theta = 42^\circ$. Data summaries below are mean values of T_{corr} plus or minus the SD for a group of cells. Increased cholesterol: $T_{\text{corr}} = 100 \pm 16$ ms (8 cells). Normal cholesterol: $T_{\text{corr}} = 65 \pm 24$ ms (8 cells). $p < 0.025$. Similar results were found for a separate preparation of similar sample.

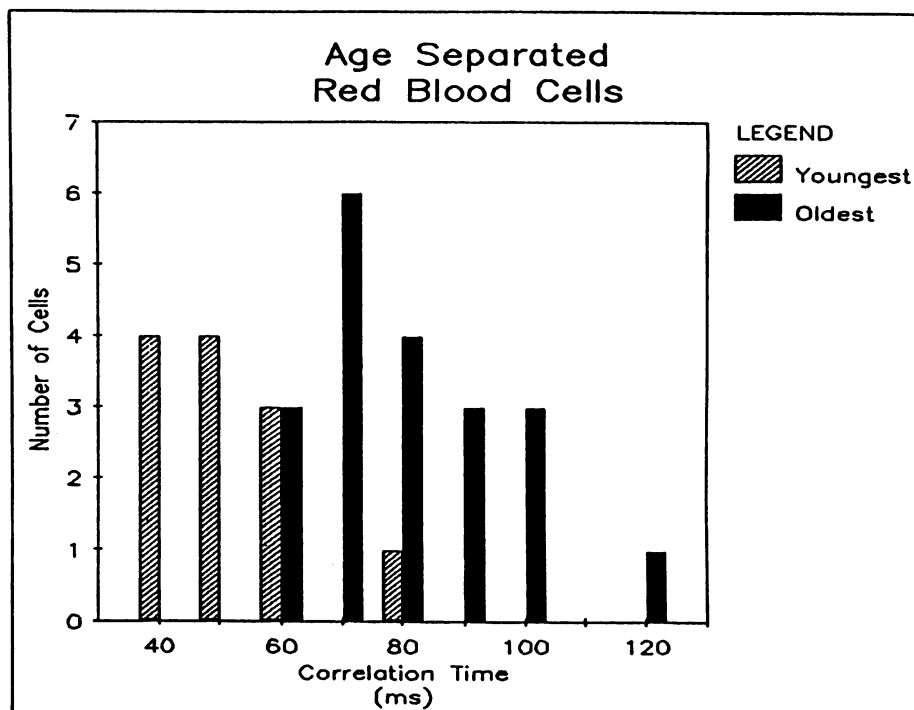


group of ghosts are slightly increased relative to that of intact RBCs, which is also evident in some of the individual data sets. An increase in the average value of T_{corr} is seen that would be expected if the faster contribution of the Hb were no longer present. However, an alternative explanation for this result, which we favor, is that the process of forming a ghost leads to changes in the membrane/cytoskeleton which cause an increase in T_{corr} . In support of this are data collected using a 1-ms sample time (which probe time scales where only the membrane/cytoskeleton could be contributing),

which show that T_{corr} for the ghosts was increased relative to that measured from the RBCs.

Power spectrum analysis of the QELS signal from human RBCs is presented in Fig. 2. This technique allowed a wider range of time scales to be included in a single data set, but also limited the high-frequency (short delay time) components that could be analyzed. The data show a complex signal made up of a wide range of frequency components with the largest contribution coming at low frequency. The apparent half-width of the low-frequency peak decreases as the sample

FIGURE 5 Distribution of correlation times for different aged red blood cells. Histograms of correlation times for youngest and oldest cells in a population of RBCs obtained using a density centrifugation separation procedure. Data shown in the histograms were obtained as described in Fig. 4. Youngest cells: $T_{\text{corr}} = 57 \pm 10$ ms (12 cells). Oldest cells: $T_{\text{corr}} = 84 \pm 16$ ms (21 cells). $p < 0.001$. Similar results (with the same p value) were found for a separate preparation of a different sample.



time is increased (Fig. 2), which is the power spectrum analogue of the mean value of T_{corr} changing as a function of sample time. The inclusion of the "white noise" level shows that the largest contributions to the power spectra are present up to the highest frequencies measured (500 Hz), as expected from the autocorrelation data.

Power spectrum analysis facilitates comparisons of the QELS data with that obtained using other spectroscopic techniques. Spontaneous motion of the RBC membrane was first observed approximately 100 years ago (Browicz, 1890) and was subsequently termed "the flicker phenomenon" (Blowers et al., 1950). The small number of quantitative studies of this phenomenon (Fricke et al., 1986; Sackmann et al., 1984; Fricke and Sackmann, 1984; Brochard and Lennon, 1975; Burton et al., 1968) have used quantitative phase contrast microscopy (Brochard and Lennon, 1975), which measures the power spectrum of thickness fluctuations in RBCs. The results of these studies have shown that the power spectrum of the motion is a monotonically decreasing function of frequency which does not extend above 25–40 Hz. Quantitative microscopy differs from QELS in that: (a) a polychromatic light source is used, (b) scattered light is collected over a wide range of scattering angles, and (c) fluctuations in the RBC thickness are measured directly.

Brochard and Lennon (1975) proposed two theoretical approaches to explain the flicker spectroscopy data. They modeled the RBC as two $8 \times 8 \mu\text{m}$ square planar bilayers separated by $2 \mu\text{m}$. They examined the contributions resulting from fluctuations in the individual bilayers, as well as squeezing modes in which motion of the two bilayers was coupled. The data they collected on human, frog and chicken RBCs agreed with their proposed model with the fluctuations arising from the "squeezing modes." The power spectra de-

creased monotonically with frequency and over the range of 1 to 30 Hz decreased as (frequency) $^{-4/3}$. The quantitative microscopy technique has been used by Fricke and Sackmann (1984) who found that the power spectrum decreased as (frequency) $^{-2}$ at higher frequencies. The difference in frequency dependence was attributed to the different manner in which the two groups treated the baseline levels of the spectra. It should be noted that in both cases, the high frequency cutoff was less than 50 Hz. Fricke and Sackmann also showed that the data could be approximated by two Lorentzians which they interpreted as evidence that there is a contribution from both the cytoskeleton and the membrane.

The overall similarity of the data obtained using the flicker spectroscopy technique and QELS is quite striking, particularly in light of the differences described above. The wide range of frequencies included in the QELS spectra also suggest that the other analyses may have underestimated the high-frequency components as well as altered the shape of the curve due to the effect of spectral aliasing related to the arbitrary high-frequency cutoff.

In one limit of the RBC model, the fluctuation modes are determined by single-membrane dynamics, which predicts specific characteristics of the QELS signal. QELS studies have been done on free surfaces, monolayers, and bilayers where fluctuations arise from a similar mechanism (Crilly and Earnshaw, 1983). The physical properties of the surfaces have been described theoretically and are in good agreement with experimental results. Application of this theory to the Brochard and Lennon model of the RBC shows that the characteristic time scales of motion due to surface waves on the RBC membrane is less than $1 \mu\text{s}$ for typical values of the physical properties of the RBC membrane (H. Z. Cummins, personal communication). This is clearly not contributing

significantly to the QELS or quantitative microscopy measurements made on the RBC.

Another possible etiology of the QELS signal is coupled motion of the two membranes (in the model) which corresponds to shape deformations of the RBC. The analysis of Brochard and Lennon showed that the range of relaxation times from these modes was ~ 50 ms to 10 s. However, their theory predicts a strong dependence on the scattering vector q (proportional to q^6) for these modes, and our data are essentially q independent.¹ A possible explanation for these modes making some contribution to the q -independent QELS signal relates to the RBC geometry. The surface of the RBC is not planar, leading to difficulty in precisely defining the scattering vector which may cause the deformation modes to be mixed together and the resultant signal being independent of q (P. G. de Gennes, personal communication). An analytical theory of membrane fluctuations that explicitly includes the RBC shape has been presented by Peterson (1985). His theory predicts that the QELS signal exhibits a weak dependence on q , which is consistent with the results presented here and with the suggestion that q independence would be expected from the RBC. Although Peterson's theory agrees with our results from single RBCs resting on a microscope slide, his own data on suspended RBC populations do not follow his theory.

Recent studies of membrane fluctuations in RBCs have shown similar spectral data which was obtained using a new optical technique based on direct measurement of amplitude fluctuations (Krol et al., 1990; Levin and Korenstein, 1991). These data suggest an interrelationship between a metabolic component of the fluctuations, which act via coupling/uncoupling of the cytoskeleton to the membrane, and the inherent physical properties of the membrane. In agreement with the QELS studies, the data on intact RBCs and ghosts are quite similar (Levin and Korenstein, 1991).

Light-scattering considerations

Calculation of the amplitude of $g^{(2)}(\tau)-1$ can give important information on the origin of the scattered light. Measurements for RBCs showed amplitudes (Fig. 1 and Table 1) much less than both the theoretical predictions (Saleh, 1978) for our experimental geometry and experimentally determined values. In previous RBC studies, the data have been normalized so that the first data channel is arbitrarily set equal to 1 (Tishler and Carlson, 1987; Blank et al., 1987; Nishio et al., 1983, 1985; Peetermans et al., 1986). The probable etiology of the decrease in $g^{(2)}(0)-1$ is the presence of elastically scattered light at the detector, an effect known as heterodyning. Elastically scattered light may arise from slowly moving or stationary regions of the RBC or possibly the scattering chamber. The contribution of a heterodyne

component in QELS from RBCs has been raised (Kam and Hofrichter, 1986), but only in the context of static scattering from gelled sickle Hb. These data show it is present in scattering from a normal RBC without any contribution from a gel.

The maximum values of $g^{(2)}(0)-1$ were measured with the shortest sample times and decreased as the sample time was increased (Table 1), as would be expected from a complex signal with many time components present. The value of $g^{(2)}(0)-1$ for the RBCs decreased as the scattering angle was decreased. The intensity of light elastically scattered from the RBC increases at smaller scattering angles (Meyer, 1979) leading to a larger heterodyne effect. Therefore, this angular dependence is consistent with heterodyning as the origin of the decreased amplitudes. Using the maximum values, $g^{(2)}(0)-1$ from a RBC is decreased relative to the amplitude of $g^{(2)}(0)-1$ from a model system of polystyrene by 7 to 25 times. If the decrease were entirely due to heterodyning, it would imply that the ratio of elastically to quasi-elastically scattered light at the detector was between 10 and 70 (Oliver, 1974). The relative mix of static versus fluctuating component appears to change with angle based on the value of the amplitude, but T_{corr} shows much less change than the amplitude. This is not unexpected since T_{corr} is less sensitive to the extent of heterodyning than is the amplitude (Oliver, 1974).

Experimental considerations

We have previously considered the potential role of artifacts arising from cell motion and external vibration; experiments with polylysine and glutaraldehyde fixation showed no contribution from these factors (Tishler and Carlson, 1987; Blank et al., 1987). Since the QELS experiments use relatively high light power densities (typically 10–30 W/cm²) compared with those used for standard phase microscopy (~ 0.01 W/cm²), the potential contribution of laser heating and sample damage needs to be considered.

Heating effects in laser studies of biological samples have been addressed both theoretically and experimentally. Piddington and Sattelle used power densities of ~ 1 W/cm² to study locust ganglia (Piddington and Sattelle, 1975; Sattelle and Piddington, 1975). They measured temperature increases for this power density and for power densities 25 times as high. The maximum temperature increase was in the range of 1–2°C (Sattelle and Piddington, 1975). The temperature effects for the RBC are less than this because the RBC has a larger surface to volume ratio than the multicellular ganglion system and should dissipate heat more efficiently. Earnshaw and Steer (1979) treated the heating effect theoretically. They assumed: (a) a 10- μm radius sphere, (b) 10% power absorption, and (c) heat loss by conduction only. With an incident power of 1 mW (~ 300 W/cm²), the temperature rise in water would be about 0.1°C. As in the previous case, the RBC experimental conditions are more favorable than this. The RBC is a biconcave disc of 8- μm diameter and therefore has a larger surface-to-volume ratio than a 10- μm

¹ q , which is called the scattering vector, is defined as $q = 4\pi n \sin(\theta/2)/\lambda$, where λ is the wavelength of light, θ is the scattering angle, and n the refractive index.

diameter sphere. In addition, less than 10% of the incident radiation was absorbed. Hb has a relatively low absorption coefficient at a wavelength of 6328 Å (Lemberg and Legge, 1949), and the thickness of the RBC is $\sim 2 \mu\text{m}$. Therefore, with the experimental conditions used for the RBC experiments, heating of the sample should not have been a contributing factor.

Observations on F-actin solutions in this laboratory (Montague, 1985) have shown that even for wavelengths where sample absorption and heating were not detectable, a perturbation of the sample due to the laser light was found. These effects were eliminated by decreasing the incident laser power density from 600 to 1 W/cm². For RBCs, power densities of 3 to 100 W/cm² showed only small differences for experiments which maintained a similar number of background counts. Further studies suggested that the differences were due to the different experiment durations rather than the power densities used. In addition, the effect seen by Montague (1985) depended on the time of exposure to the laser beam. The RBC experiments were typically 5 min long, while the effects on actin were seen only after exposure of an hour or more.

Species studies

In our initial presentation of the RBC data, a biological "control," the human white blood cell (WBC) was examined (Tishler and Carlson, 1987). The WBC, which differs from the RBC in terms of size, shape, cytoplasmic viscosity, cellular components and myriad of other ways, was studied in order to see if a QELS signal of significantly different character were found. The large WBC with its more viscous cytoplasm demonstrated a signal with a significantly longer decay time. We present here the results from a complementary biological study in which a variety of RBCs from other species were examined, with the expectation that those with similar structures would have signals similar to the human RBC.

The spontaneous motion of the RBC membrane/cytoskeleton presumably is related to the physical structure of the membrane/cytoskeleton, as opposed to the precise biochemical constituents of the cytoplasm. Consequently, results comparable to the human RBC would be expected in cells with a similar structure. There was no significant difference between data from anucleate mammalian RBCs which included a wide variety of species (Table 5). This similarity was observed in spite of the fact that there were substantial differences between the biochemical constituents of the cells. For example, the human RBC has a high intracellular potassium concentration (greater than 100 mM; Beulter and Srivastava, 1977) while for a dog RBC the potassium concentration is approximately 10 mM (Ponder, 1941). Similarly, the QELS signal would be expected to differ for cells which differed structurally from the mammalian RBC, as was previously demonstrated for the human WBC. Data from nucleated RBCs are included in Table 5. In addition to having a nucleus, the toad RBC ($10\text{--}15 \times 20\text{--}25 \mu\text{m}$) and chicken RBC ($6 \times 12 \mu\text{m}$) differed in both size and

TABLE 5 Correlation times for red blood cells from different species

Type of cells	Cell size (μm)	T_{corr} (ms)
Human	7–8	65 ± 24 (8) 60 ± 18 (8) 56 ± 20 (15)
Dog	7	63 ± 15 (14)
Rat	5–6.5	61 ± 12 (9)
Beluga whale	6.5–7	
Anore		66 ± 11 (7 of 8)
Illamar		68 ± 25 (7 of 8)
Harbor seal	5.5–7.5	
Danny		57 ± 12 (8 of 9)
Orange		69 ± 10 (9 of 10)
Jungle cat	5.5–7.5	53 ± 13 (9)
Antelope	4.5–5.5	79 ± 23 (9 of 10)
Chicken*	7 × 12	127 ± 33 (12)
Toad*	13 × 19	185 ± 75 (11 of 12)

Summary of autocorrelation data measured from RBCs of different species. Each set of human RBC data was taken from different preparations. Data from nucleated cells were collected from a region including the nucleus. Criteria for accepting data from a particular cell are the same as those used for the RBC ghosts. Values for the size of chicken RBCs were obtained from Lucas and Jamroz (1961) and values for the toad from Andres (1965). Other values were found in Archer and Jeffcoat (1977). Data from the chicken and toad RBCs were significantly different from the human samples. There was no difference between the data from the other species and the human RBCs. $\theta = 42^\circ$; sample time = 1 ms.

* Nucleated RBC.

shape from the mammalian cells. Measurements of $g^{(2)}(\tau)$ from these cells were compared with measurements from human RBCs and T_{corr} was increased in the nucleated RBCs. The measurements were made with the standard microscope equipment and thus the cross sectional diameter of the scattering volume was approximately 8 μm . In experiments on the chicken RBC, the region of the cell contained in the scattering volume included the nucleus and the lateral edges of the cell. For the toad RBCs, separate measurements were made in the region of the nucleus and the edge of the cell, but the values of T_{corr} from these two regions did not differ significantly. There was, however, a significant increase in the scattered intensity from edge of the cell compared with the region of the nucleus. In addition, the value of $g^{(2)}(0)-1$ was increased in the region of the nucleus. The scattering intensity from the edge of the toad RBC was comparable to that from the human RBC, suggesting that for the human RBC the edge of the cell made a large contribution to the total scattered intensity.

The effect of increased cytoplasmic viscosity on the QELS signal from red blood cells

Increasing the osmotic strength of the RBC buffer led to a decrease in the intracellular water content which resulted in an increase in the cytoplasmic protein concentration (McConaghey and Maizels, 1961). Experiments which used different ionic compounds demonstrated that these changes were specifically osmotic effects and were not due to changes in ionic strength or specific ions (Table 3). Increases in cytoplasmic viscosity have been independently shown to decrease the spontaneous motion of the RBC membrane (Colletta et al., 1982; Padilla et al, 1973).

Previous measurements of the effect of increased viscosity on spontaneous RBC membrane motion examined the effect of polymerization of sickle cell Hb within RBCs. In a study of sickle cells Padilla et al. (1973) noted that the flicker phenomenon ceased as the Hb polymerized, even prior to sickling of the RBC. During the phase of deoxygenation prior to morphological changes of the cell, polymerization of the sickle Hb led to an increase in cytoplasmic viscosity. A similar observation was made in studies of the scattered light intensity from sickle RBCs during the process of Hb polymerization. Fluctuations in the scattered intensity, which were attributed to flicker motion of the cell membrane, decreased as the mean scattered intensity increased due to the formation of Hb polymers (Coletta et al., 1982). Measurements of the polymerization of concentrated sickle cell Hb in solution did not exhibit these fluctuations in scattering intensity (Ferrone et al., 1980). Decreases in the intensity fluctuations of light scattered from sickle cell RBCs were also measured using QELS (Nishio et al., 1983). Although these changes were attributed to decreases in the Hb diffusion coefficient, the decreased membrane motion accounts for this result.

Increasing the osmotic strength of the buffer and increasing cytoplasmic viscosity has also been shown to decrease cell deformability. Studies of RBC filterability with a variety of pore sizes showed decreases in RBC deformability with increasing osmotic strength (Reinhart and Chien, 1985). Micropipette aspiration studies showed that the dynamic rigidity of the RBC increased as Hb concentration increased, while the static properties were unchanged (Evans et al., 1984). These studies demonstrate that RBCs with increased cytoplasmic viscosity have changes in their dynamic properties and are less deformable. QELS measurements on the less deformable cells showed increases in T_{corr} . These findings are consistent with the data presented below where decreased cell deformability was induced by direct manipulation of the membrane/cytoskeleton complex.

Biochemical modifications of the red blood cell membrane/cytoskeleton

Two biochemical manipulations which primarily act on the membrane/cytoskeleton of the RBC were studied in order to determine their effect on the QELS signal. Increasing the membrane cholesterol content and increasing the intracellular calcium concentration both lead to decreased deformability of the cells, as assessed in a number of different ways. The goal of these studies was to determine if QELS was sensitive to biochemically induced changes in the membrane/cytoskeleton.

A. Calcium effect

Increased intracellular calcium levels have been shown to decrease the deformability of the human RBC. These changes have been measured using ektacytometry (Heath et al., 1982), micropipette aspiration techniques (Smith et al., 1981) and a filtration assay (O'Rear et al., 1982). The change

in deformability has been attributed to different mechanisms: 1) direct effects on the intrinsic properties of the membrane/cytoskeleton and 2) intracellular dehydration secondary to potassium efflux which leads to increased cytoplasmic viscosity. If the ionophore A23187 is used to alter the intracellular Ca^{2+} levels and manipulations are performed in a high potassium buffer (as they were here) the dehydration effects are minimized (Heath et al., 1982) and the predominant effect is that of calcium acting on the membrane/cytoskeleton. Increased intracellular calcium has been associated with intrinsic changes of the membrane/cytoskeleton but no other significant changes in the physical properties of the cell (O'Rear et al., 1982). Increased intracellular calcium levels lead to changes of the RBC shape and formation of a high molecular weight complex which consisted of cross-linked cytoskeletal proteins (Lorand et al., 1978). Polymer formation was inhibited under conditions in which the changes in deformability were also inhibited, suggesting that the enzymatic cross-linking of the cytoskeletal proteins may be the cause of the membrane changes (Siefing et al., 1978).

The QELS signal was altered significantly in cells which had increased intracellular calcium levels (Table 4). T_{corr} was increased in the presence of increased calcium, independent of cell morphology; statistically insignificant increases were observed for cells with echinocytic morphology. Controls with magnesium replacing the calcium in the buffer or without the presence of a divalent cation had lower values of T_{corr} than the calcium treated cells which had significant changes in their QELS signal, characterized by increases in T_{corr} .

B. Cholesterol effect

Increasing the cholesterol level of the RBC membrane leads to a decrease in fluidity as measured by a fluorescent probe which partitions into the membrane (Cooper et al., 1978). Cell deformability was shown to decrease as the C/P ratio increased using both the filtration assay (Cooper et al., 1975) and micropipette aspiration of an entire cell (Shiga et al., 1979).

The QELS studies comparing cholesterol loaded cells with controls showed a clear increase in T_{corr} for the cells with increased cholesterol levels (Figs. 3 and 4). This indicated that changes in the composition of the cell membrane which led to decreased deformability of the cell led to changes in the QELS signal. This result is consistent with the data obtained in the calcium studies where the less deformable cells showed an increase in T_{corr} .

Physiologic changes in membrane properties

During the 120 days that the human RBC spends in the bloodstream, it undergoes changes which eventually lead to its destruction. The precise mechanism leading to the removal of aged cells by the reticulo-endothelial system has not been identified, but it is generally believed that an important contribution is the decreasing deformability of the cell as it ages (Sutera et al., 1985). The deformability of aged RBCs has been shown to decrease by micropipette aspiration studies

(Nash and Wyard, 1981; Linderkamp and Meiselman, 1982; Nash and Meiselman, 1983), experiments on cells subjected to shear stresses (Sutera et al., 1985) and changes in filtration times (Tillman et al., 1980). These studies have shown that the membrane viscosity of the RBC increases significantly with age, which leads to slower recovery times as its shape is altered (Linderkamp and Meiselman, 1982; Nash and Meiselman, 1983). The RBC density also increases as the cell ages due to water loss. This contributes to the decreased deformability through an increase in cytoplasmic viscosity. However, the overall decrease in deformability arises primarily from the increased membrane viscosity with the increased cytoplasmic Hb concentration making a lesser contribution (Linderkamp and Meiselman, 1982; Nash and Meiselman, 1983; Sutera et al., 1985).

As shown in Fig. 5, there is a significant difference between the values of T_{corr} for the oldest and youngest cells in a RBC population. T_{corr} was increased in the older, less deformable cells relative to the younger more deformable ones. This indicates that changes in the spontaneous dynamic properties of the RBC membrane can be measured for age separated RBC populations. This age-dependent change in the QELS signal is consistent with the previously studied examples where the less deformable cells showed increased values of T_{corr} . This demonstrates that physiologic, as well as biochemically induced, changes in the deformability of the membrane/cytoskeleton of single human RBCs can be monitored using QELS.

SUMMARY

QELS spectroscopy has been applied to the study of individual human RBCs and data were analyzed using autocorrelation functions and power spectra. Both approaches showed that a broad range of correlation times or frequency components were present. The precise values calculated for T_{corr} were a strong function of the sample time used. Anucleate, mammalian RBCs had QELS signals similar to the human RBC, regardless of their cellular diameters or precise ionic compositions. T_{corr} was increased for nucleated oval shaped RBCs, further suggesting an origin of the signal from the physical/mechanical properties of the membrane/cytoskeleton and its associated spontaneous fluctuations.

The effects of biochemical modifications of the membrane/cytoskeleton were examined. Increasing the membrane cholesterol to phospholipid ratio and increasing the intracellular calcium concentration have been shown to decrease the deformability of the RBC. In both experiments, RBCs which were made less deformable had increased values of T_{corr} . This result gave further support to the membrane/cytoskeleton as the primary source of the QELS signal and showed that QELS could be used to measure changes of the physical properties of the membrane/cytoskeleton. Deformability of the RBC refers to its response to shape deformation and is determined by cell geometry, cytoplasmic viscosity, membrane rheological properties, and interactions between all three of these (Chien, 1987). T_{corr} was increased for cells

in buffers with increased osmotic strengths, indicating that the increased cytoplasmic viscosity led to a slowing of the motion of the membrane/cytoskeleton. Older RBCs, which are less deformable, had increased values of T_{corr} relative to younger cells. In the same way that the artificially induced decreases in deformability led to increased values of T_{corr} , physiological decreases in deformability, which occur in older RBCs relative to younger ones, also led to increases in T_{corr} . This demonstrated that QELS can be used to measure physiological changes of the membrane/cytoskeleton.

The relatively simple structure of the human RBC has allowed the membrane/cytoskeleton to be identified as the primary source of the QELS signal (Tishler and Carlson, 1987). This association will allow studies to be made on further biochemical alterations of the cell as well as the effect of other physiological or pathological changes. The change of various physical parameters can be studied in conjunction with QELS and aid in the synthesis of a theory for the precise physical basis for the QELS signal, which was not developed here. In addition to the intrinsic interest of the RBC, it can serve as a model for studying membrane motion in other cell systems. The intrinsic fluctuations of cell membranes in general—its physical and theoretical basis as well as its biological implications—are currently a subject of much interest (Krol et al., 1990; Levin and Korenstein, 1991; Lipowsky, 1991), a subject that these data and this technique can play a role in elucidating.

Many previous QELS studies of individual cells have focused on studying motion of cytoplasmic inclusions or intrinsic properties of the cytoplasm (Shaw and Newby, 1972; Englert, 1980; Englert and Edwards, 1977; Piddington and Satelle, 1975; Satelle and Piddington, 1975; Nishio et al., 1983, 1985, Peetermans et al., 1986). The present work demonstrates that membrane motion may make a contribution in studies of cytoplasmic inclusions or diffusive processes and that these contributions must be considered in the analysis of QELS data from single cells. On another level, however, it demonstrates that QELS is a potentially valuable technique for studying intrinsic membrane properties in individual cells.

We thank J. Baltz, P. S. Blank, H. Z. Cummins, J. Earnshaw, P. G. de Gennes, and C. E. Montague for helpful comments and discussions. We would also like to thank Dover Poultry Co., the National Aquarium in Baltimore, the Baltimore Zoo, B. Mangold, and B. A. Simon for assistance in obtaining the blood samples from different species.

This work was supported by National Institutes of Health grant 5 RO1 AM12803-26 (awarded to F. D. C.). R. B. T. was supported by Medical Scientist Training grant 5 T32 GM07309.

REFERENCES

- Andrew, W. 1965. *Comparative Hematology*. Grune and Stratton, Inc., New York.
- Archer, R. K., and L. B. Jeffcott, eds. 1977. *Comparative Clinical Hematology*. Blackwell Scientific Publications, Oxford.
- Beutler, E., and S. Srivastava. 1977. Composition of the erythrocyte. *In Hematology*. W. Williams and E. Beutler et al., editors. McGraw-Hill, New York. 135–141.

- Blank, P. S., R. B. Tishler, and F. D. Carlson. 1987. Quasi-elastic light scattering microscope spectrometer. *Appl. Optics*. 26:351–356.
- Blank, P. S., R. B. Tishler, and F. D. Carlson. 1986. Quasi-elastic light scattering studies of single cells using a microscope spectrometer. *Proc. SPIE*. 712:166–171.
- Bloomfield, P. 1976. The spectrum. In *Fourier Analysis of Time Series: An Introduction*. Wiley and Sons: New York. 151–179.
- Blowers, R., E. M. Clarkson, and M. Maizals. 1950. Flicker phenomenon in human erythrocytes. *J. Physiol.* 113:228–239.
- Brochard, F., and J. F. Lennon. 1975. Frequency spectrum of the flicker phenomenon in erythrocytes. *J. Physique*. 36:1035–1047.
- Browicz, V. 1890. Weitere beobachtunger uber bewegungsphanomene an roten blutkorperchen in pathologischen zustanden. *Zbl. Med. Wiss.* 28: 625–627.
- Burton, A., L. Anderson, and R. Andrews. 1968. Quantitative studies on the flicker phenomenon in the erythrocytes. *Blood*. 32:819–822.
- Chien, S. 1987. Red cell deformability and its relevance to blood flow. *Annu. Rev. Physiol.* 49:177–192.
- Cochran, W. G. 1964. Approximate significance levels of the Behrens-Fisher test. *Biometrics*. 20:191–195.
- Coletta, M., J. Hofrichter, F. Ferrone, and W. Eaton. 1982. Kinetics of sickle haemoglobin polymerization in single red cells. *Nature Lett.* 300:194–197.
- Cooley J., P. Lewis, and P. Welch. 1977. The fast Fourier transform and its application to time series analysis. In *Mathematical Methods for Digital Computers*. Vol. 3. Statistical Methods for Digital Computers. K. Endein, A. Ralston, and H. S. Wolf, editors. Wiley, New York. 377–423.
- Cooper, R., E. Arner, J. Wiley, and S. Shattil. 1975. Modification of red cell membrane structure by cholesterol-rich lipid dispersions. *J. Clin. Invest.* 55:115–126.
- Cooper, R. A., M. H. Leslie, S. Fischkoff, M. Shinitzky, and S. J. Shattil. 1978. Factors influencing the lipid composition and fluidity of red cell membranes in vitro: Production of red cells possessing more than two cholesterol per phospholipid. *Biochemistry*. 17:327–331.
- Crilly, J. F., and J. C. Earnshaw. 1983. Photon correlation spectroscopy of bilayer lipid membranes. *Biophys. J.* 41:197–210.
- Earnshaw, J., and M. Steer. 1979. Studies of cellular dynamics by laser doppler microscopy. *Pestic. Sci.* 10:358–368.
- Englert, D. 1980. An optical study of isolated rat adrenal chromaffin cells. *Exp. Cell Res.* 125:369–376.
- Englert, D., and C. Edwards. 1977. Effect of potassium concentration on particle motion with a neurosecretory structure. *Proc. Natl. Acad. Sci. USA*. 74:5759–5763.
- Evans, E., N. Mohandas, and A. Leung. 1984. Static and dynamic rigidities of normal and sickle erythrocytes. Major influence of cell hemoglobin concentrations. *J. Clin. Invest.* 73:477–488.
- Ferrone, F., J. Hofrichter, H. Sunshine, and W. Eaton. 1980. Kinetic studies on photolysis-induced gelation of sickle cell hemoglobin suggest a new mechanism. *Biophys. J.* 32:361–377.
- Ford, N. 1983. Theory and practice of correlation spectroscopy. In *Measurement of Suspended Particles by Quasi-Elastic Light Scattering*. B. Dahneke, editor. John Wiley and Sons, Inc., New York.
- Fricke, K., and E. Sackmann. 1984. Variation of frequency spectrum of the erythrocyte flickering caused by aging osmolarity, temperature and pathological changes. *Biochim. Biophys. Acta*. 803:145–152.
- Fricke, K., K. Wirthenson, R. Laxhuber, and E. Sackmann. 1986. Flicker spectroscopy of erythrocytes. A sensitive method to study subtle changes of membrane bending stiffness. *Eur. Biophys. J.* 14:67–81.
- Haskell, R., and F. D. Carlson. 1981. Quasi-elastic light scattering studies of single skeletal muscle fibers. *Biophys. J.* 33:39–62.
- Heath, B., N. Mohandas, J. Wyatt, and S. Shohet. 1982. Deformability of isolated red blood cell membranes. *Biochim. Biophys. Acta*. 691:211–219.
- Hoerber, R. 1945. *Physical Chemistry of Cells and Tissues*. The Blakiston Company, Philadelphia.
- Hui, S., C. Stewart, M. Carpenter, and T. Stewart. 1980. Effects of cholesterol on lipid organization in human erythrocyte membranes. *J. Cell Biol.* 85:283–291.
- Jacobs, M., and D. Stewart. 1947. Osmotic properties of the erythrocyte: XII. Ionic and osmotic equilibria with a complex external solution. *J. Cell. Comp. Phys.* 30:79–103.
- Jakeman, E., C. J. Oliver, E. R. Pike, and P. N. Pusey. 1972. Correlation of scaled photon-counting fluctuations. *J. Phys. A: Gen. Phys.* 5:L93–L96.
- Jones, R. 1962. Spectral analysis with regularly missed observations. *Ann. Math. Statist.* 33:455–461.
- Kansu, E., S. Krasnow, and S. Bassas. 1980. Spectrin loss during in vitro red cell lysis. *Biochim. Biophys. Acta*. 596:18–27.
- Kam, Z., and J. Hofrichter. 1987. Quasi-elastic light scattering from solutions and gels of hemoglobin. *Biophys. J.* 50:1015–1020.
- Krol, A. Y., M. G. Grinfeldt, S. V. Levin, and A. D. Smilgavichus. 1990. Local mechanical oscillations of the cell surface within the range 0.2–30 Hz. *Eur. Biophys. J.* 19:93–99.
- Lemberg, R., and J. W. Legge. 1949. *Hematin Compounds and Bile Pigments: Their Constitution, Metabolism, and Function*. Interscience Publishers, Inc., New York.
- Levin, S., and R. Korenstein. 1991. Membrane fluctuations in erythrocytes are linked to MgATP-dependent dynamic assembly of the membrane skeleton. *Biophys. J.* 60:733–737.
- Lin, S., and C. Snyder. 1977. High affinity cytochalasin B binding to red cell membrane proteins which are unrelated to sugar transport. *J. Biol. Chem.* 252:5464–5471.
- Linderkamp, O., and H. Meiselman. 1982. Geometric, osmotic, and membrane mechanical properties of density-separated human red cells. *Blood*. 59:1121–1127.
- Lipowsky, R. 1991. The conformation of membranes. *Nature (Lond.)*. 349: 475–481.
- Lorand, L., G. Siefbrig, and L. Lowe-Krentz. 1978. Formation of γ -glutamyl-e-lysine bridges between membrane proteins by a Ca^{2+} -regulated enzyme in intact erythrocytes. *J. Supramol. Struct.* 9:427–440.
- Lucas, A. M., and Jamroz, C. 1961. *Atlas of Avian Hematology*. U.S. Department of Agriculture, Washington, DC.
- McConaghey, P. D., and M. Maizels. 1961. The osmotic coefficients of haemoglobin in red cells under varying conditions. *J. Physiol.* 155:28–45.
- Meyer, R. 1979. Light scattering from biological cells: dependence of backscatter radiation on membrane thickness and refractive index. *Appl. Opt.* 18:585–588.
- Montague, C. 1985. A study of the polydispersity of F-actin by photon correlation spectroscopy; including an extension of the exponential sampling method using a rigid rod model. Ph.D. thesis, Johns Hopkins University, Baltimore, Maryland.
- Morton, G. A., H. M. Smith, and R. Wasserman. 1967. Afterpulses in photomultipliers. *Trans. Nucl. Sci.* NS-14:443–448.
- Nash, G., and H. Meiselman. 1983. Red cell and ghost viscoelasticity. Effects of hemoglobin concentration and in vivo aging. *Biophys. J.* 43:63–73.
- Nash, G., and S. Wyard. 1981. Erythrocyte membrane elasticity during in vivo aging. *Biochim. Biophys. Acta*. 643:269–275.
- Nishio, I., J. Peetermans, and T. Tanaka. 1985. Microscope laser light scattering spectroscopy of single biological cells. *Cell. Biophys.* 7:91–105.
- Nishio, I., T. Tanaka, Y. Imanishi, S. Ohnishi. 1983. Hemoglobin aggregation in single red blood cells of sickle cell anemia. *Science (Washington DC)*. 220:1173–1175.
- Oliver, C. J. 1974. Correlation techniques. In *Photon Correlation and Light Beating Spectroscopy*. H. Z. Cummins and E. R. Pike, editors. Plenum Press, New York. 151–223.
- O'Rear, E., M. Udden, L. McIntire, and E. Lynch. 1982. Reduced erythrocyte deformability associated with calcium accumulation. *Biochim. Biophys. Acta*. 691:274–280.
- Padilla, F., P. Bromberg, and W. Jensen. 1973. The sickle-unsickle cycle: a cause of cell fragmentation leading to permanently deformed cells. *Blood*. 41:653–660.
- Parzen, E. 1963. On spectral analysis with missing observations and amplitude modulation. *Sankhya A*. 25:383–392.
- Peterson, M. 1985. Shape fluctuations of red blood cells. *Mol. Cryst. Liq. Cryst.* 127:159–186.
- Peetermans, J., I. Nishio, S. T. Ohnishi, and T. Tanaka. 1986. Light-scattering study of depolymerization kinetics of sickle hemoglobin polymers inside single erythrocytes. *Proc. Natl. Acad. Sci. USA*. 83:352–356.
- Piddington, R., and D. Sattelle. 1975. Motion in ganglia detected by light-beating spectroscopy. *Proc. R. Soc. Lond. B*. 190:415–420.

- Ponder, E. 1948. Hemolysis and Related Phenomena. Grune and Stratton, New York.
- Reinhart, W., and S. Chien. 1985. Roles of cell geometry and cellular viscosity in red cell passage through narrow pores. *Am. J. Physiol.* 248 (*Cell Physiol.* 17:C473-C479).
- Sackmann, E., J. Englehardt, K. Fricke, and H. Gaub. 1984. On dynamic molecular and elastic properties of lipid bilayers and biological membranes. *Coll. Surf.* 10:321-335.
- Saleh, B. 1978. Photoelectron Statistics With Applications to Spectroscopy and Optical Communications. Springer-Verlag, New York.
- Sattelle, D., and R. Piddington. 1975. Potassium-induced motion increase in a central nervous ganglion. *J. Exp. Biol.* 62:753-770.
- Schindler, M., D. Koppel, and M. Sheetz. 1980. Modulation of membrane protein lateral mobility by polyphosphates and polyamines. *Proc. Natl. Acad. Sci. USA.* 77:1457-1461.
- Shaw, T. I., and B. J. Newby. 1972. Movement in a ganglion. *Biochem. Biophys. Acta.* 255:411-412.
- Sheif, R. F., and P. C. Wensink. 1981. Practical Methods in Molecular Biology. Springer-Verlag, New York.
- Shiga, T., N. Maeda, T. Suda, K. Kon, M. Sekiya, and S. Oka. 1979. Rheological and kinetic dysfunction of the cholesterol loaded, human erythrocytes. *Biorheology.* 16:363-369.
- Siefring, G., A. Apostol, P. Velasco, and L. Lorand. 1978. Enzymatic basis for the Ca^{2+} -induced cross-linking of membrane proteins in intact human erythrocytes. *Biochemistry.* 17:2598-2604.
- Smith, B., P. LaCelle, G. Siefring, L. Lowe-Krentz, and L. Lorand. 1981. Effects of the calcium-mediated enzymatic cross-linking of membrane proteins on cellular deformability. *J. Membr. Biol.* 61:75-80.
- Snedecor, G., and W. G. Cochran. 1967. Statistical Methods. Iowa State University Press, Ames, Iowa.
- Sutera, S., R. Gardner, C. Boylan, K. Carroll, K. Chang, J. Marvel, C. Kilo, and J. Williamson. 1985. Age-related changes in deformability of human erythrocytes. *Blood.* 65:275-282.
- Tanaka, K., and S. Ohnishi. 1976. Heterogeneity in the fluidity of intact erythrocyte membrane and its homogenization upon hemolysis. *Biochim. Biophys. Acta.* 426:218-231.
- Tillman, W., C. Levin, G. Prindull, and W. Schroter. 1980. Rheological properties of young and aged human erythrocytes. *Klin. Wochenschr.* 58:569-574.
- Tishler, R. B., and F. D. Carlson. 1987. Quasi-elastic light scattering studies of membrane motion in single red blood cells. *Biophys. J.* 51:993-997.
- Vettore, L., M. De Matteis, and P. Zampini. 1980. A new density gradient system for the separation of human red blood cells. *Am. J. Hematol.* 8:291-297.